Experimental and theoretical investigation of the microstructural evolution in aluminium alloys during extrusion

T. Kayser, F. Parvizian, B. Klusemann & B. Svendsen
Chair of Mechanics, Dortmund University of Technology, Germany

Abstract

The purpose of this work is the investigation of the microstructural evolution in aluminium alloys during extrusion at high temperature and subsequent cooling. In particular, the alloy EN AW-6060 of the 6000 series (Al-Mg-Si) is examined here. Subject to such process conditions, the microstructural development in this high stacking-fault material is controlled mainly by dynamic recovery during extrusion and static recrystallisation during cooling. To characterize this development in more detail, EBSD measurements are carried out on different parts of a partly extruded specimen. From this sample, microstructural images are generated and a statistical analysis is performed. Our initial simulation results of the microstructural development during this process show good qualitative agreement with the trends found experimentally via the EBSD investigation.
Keywords: aluminium, microstructure, extrusion, EBSD, subgrains, misorientation.

1 Introduction

Extrusion as a technological process is used to produce profiles with constant cross section from materials such as aluminium, copper, stainless steel, and various types of plastics. The advantages of aluminium and its alloys include high ductility (due to its fcc crystal structure), making it particularly suitable for complex extrusion processes. Additionally, the ideal ratio of the Young's modulus to density of aluminium allows a wide range of applications in automotive and aircraft manufacturing, as well as for lightweight construction in general.

The focus of this short work is to report on the microstructural details of an extruded EN AW-6060 alloy in order to determine the influence of various process

WIT Transactions on Engineering Sciences, Vol 64, © 2009 WIT Press
www.witpress.com, ISSN 1743-3533 (on-line)
doi:10.2495/MC090201

Table 1: Alloy composition of aluminium EN AW-6060 (components in alphabetical order)

component	Cr	Cu	Fe	Mg
%-weight	0.05	0.1	0.1-0.3	0.35-0.6
component	Mn	Si	Ti	Zn
%-weight	0.1	0.3-0.6	0.1	0.15

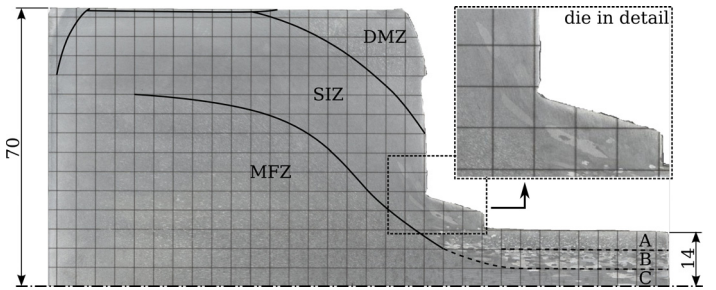

Figure 1: Partly extruded block of aluminium EN AW-6060.

parameters on the resulting microstructure. Aluminium EN AW-6060 is a commonly used industrial alloy with a composition shown in table 1. The main material characteristics are dominated by the components magnesium and silicon and their intermediate phase Mg_2Si which is responsible for the hardening behaviour of this particular alloy [1].

The investigations are performed on a partly extruded block of aluminium EN-AW-6060. After removal from the extrusion press and air cooling to room temperature, the specimen is cut along the middle axis in the extrusion direction. The cut surface is then polished and etched to reveal the grain structures which develop at different stages during the extrusion process.

Fig. 1 shows an etched cross section of the prepared partly extruded block with a block diameter of 140 mm and 28 mm in the extruding rod. The visible black grid is overlayed during the scan of the specimen. Further details about process conditions can be found in Table 2. The temperature in the container and die is determined by the extrusion press used. As indicated, it is generally lower than the initial temperature of the pre-heated block.

2 Microstructure evolution

2.1 Global microstructure overview

In the partly extruded block shown in Fig. 1, three different zones of microstructural development are evident. In the Dead Material Zone (DMZ), which forms

Table 2: Extrusion process conditions.

pre-heated block temp.	450°C
container temp.	350°C
die temp.	350°C
ram velocity	5 mm/s
extrusion ratio	5

a cone at the front of the block, friction between the block, container and die results in little material deformation and concomittant microstructural development. Indeed, the microstructure in the DMZ remains almost unchanged in its original state. In the neighbouring Shear Intensive Zone (SIZ), however, the material undergoes significant and predominantly shear deformation. As a result, the microstructural evolution in this region is quite complex, both during extrusion and cooling. The central region of the block represents the so-called Material Flow Zone (MFZ). Here, the material flows toward the centre of the extruded block. This material is mainly stretched in direction of extrusion and individual grains elongate into a banded texture [2].

Due to the high stacking fault energy of aluminum alloys such as EN AW-6060 and to the high temperature conditions during the extrusion process, the microstructure evolution, especially in the SIZ, is primary influenced by dislocation climb and dynamic recovery. The existing and additional deformation induced dislocations rearrange into dislocation-poor cells separated by low-angle dislocation-rich walls in the interior of existing grains, resulting in so-called subgrain formation. With further deformation, this results in a systematic decrease in the mean grain and subgrain size. Local shear deformation also leads to an increase of the misorientation angle between subgrains inside a grain. Misorientations larger than 15° indicate the transition from subgrain to grain. In addition, initial grain boundaries become serrated due to the subgrain evolution during grain elongation. In the extreme, this results in the joining of opposing grain boundaries to form new and smaller grains (see marked details in microstructure of point C6 in Fig. 2). Since new grains are formed in this process (at the size of the former subgrains), this mechanism is also known as geometric dynamic recrystallisation (GDX) [3]. Note that this has nothing to do with nucleation-based kinetics-driven dynamic recrystallization, which in comparison to dynamic recovery is energetically-unfavorable in aluminum alloys such as EN AW-6060 under the extrusion conditions of interest here.

The microstructure of the resulting profile can be subdivided into three zones denoted as A, B and C. The central zone C contains material from the MFZ. Here, the minimum stored energy needed to drive static recrystallisation upon extrusion is not generally attained. Consequently, on average, the deformation-dominated elongated-grain texture microstructure developed during the extrusion

process persists after the extrudate exits the die. Only in a few isolated regions near to the middle axis where the temperature stayed at a comparable high level exhibit some recrystallisation. The neighbouring Zone B evolves from the SIZ and is characterised by larger grains resulting from static recrystallisation. Apparently, sufficient energy storage takes place in the SIZ to drive recrystallisation after extrusion. Indeed, combined with faster cooling in regions near the free surface of the extrudate, this leads to recrystallisation becoming energetically more favourable than dynamic recovery. The high distortion energy in the deformed grains leads to a high-angle grain boundary migration starting at certain nuclei forming a new microstructure of dislocation free grains. More toward the interior, cooling below the critical recrystallisation temperature is slower, allowing longer growth of primarily recrystallised grains. This mechanism – called secondary recrystallisation – is now driven by the high surface energy of a fine grained microstructure. In contrast to this, zone A, which is also formed from the SIZ, shows a finer globular microstructure resulting only from primary recrystallisation. This stops when the temperature in this area near the surface drops below the critical recrystallisation temperature. The smooth transition between zones A and B is primarily temperature-related, whereas the one between zones B and C results from a sharp separation of materials from different deformation zones (SIZ and MFZ).

Taking a closer look at the microstructure near the die (see detailed view in Fig. 1) reveals elongated, abnormally large recrystallised grains in this area. This unexpected microstructure is in contradiction with the above mentioned recovery mechanism and is due to special experimental conditions. As shown in Fig. 1 the block is only partly extruded. It took 10 minutes to remove this partly extruded block from the press. During this time it remained heated. Because of this, primary and secondary recrystallisation occurs in the material from the SIZ near the die. This is not expected to occur in the block or in the die region during a continuous extrusion process.

2.2 Microstructure evolution along middle axis

The characterisation here is based on Electron Backscattering Diffraction (EBSD) measurements. These facilitate direct access to the microstructural characteristics like grain misorientation or (sub-)grain size. EBSD measurement results consist of a list of measurement point coordinates together with the Euler angles describing the orientation of the crystal lattice in space at this point. Beside using the commercial program Orientation Imaging Microscopy^{TM} (OIM), we developed and use our own software to generate images of the microstructure from the EBSD data as shown in Fig. 2. Here, the colours are directly related to lattice orientation and represent distinct grains with a relative misorientation greater than 15°. The original EBSD measurement data also contain several points where no measurement was possible, as well as fragments of over- or underlying grains which are automatically filtered out. All results to follow have been directly generated by our in-house software GRAINPLOT and have been validated via comparison with OIM.

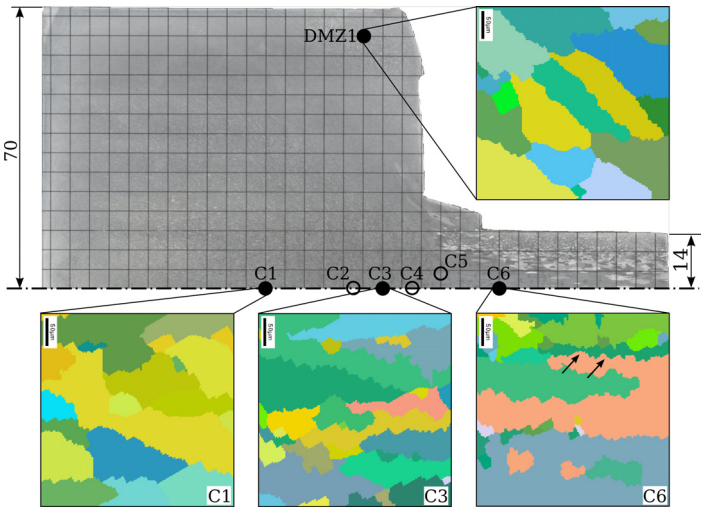

Figure 2: Microstructure evolution along middle axis.

An overview of microstructural evolution in the block is shown in Fig. 2. This is represented by four EBSD measurement points in the block along its axis together with one point in the DMZ. The microstructure of point DMZ1 in the dead material zone serves as an example of the initial microstructure in the block and as a reference for comparison with the microstructure at the other points. The three micrographs below the block in Fig. 2 illustrate the previous discussed elongation and reorientation of grains in the centre of the block. The arrows in the micrograph of point C6 mark the serrated grain boundaries which later lead to a fragmentation into separate grains of former subgrain size.

Exemplary of the general microstructural development as a whole in this region are the results at points C1, C3 and C6. C1 is 40 mm, and C3 10 mm, in front of the die inflow. Further, C6 is located 5 mm beyond the die exit. Each EBSD measurement shown covers an area of 350 x 350 µm. The EBSD results for the additional points C2, C4, and C5 are not shown; however, these results are included in the statistical characterisation of the microstructure to follow.

Beside the graphical representation of the microstructure, the EBSD method also allows a statistical evaluation regarding microstructural quantities. For example, Fig. 3 shows the development of the number of grains separated by high-angle boundaries as well as that of their mean and median grain sizes. Clearly indicated here is the decrease of mean grain size during the deformation process. The stagnation and slight increase at point C5 does not fit into this general behaviour. This could be related to the location of C5 at 3.5 mm outside the centre line for reasons of the specimen preparation. The median grain size in Fig. 3 is more robust against outliner values and confirms the general decreasing character of the grain size. Corresponding to the deceasing grain size is an increase in the number of grains along the centre line.

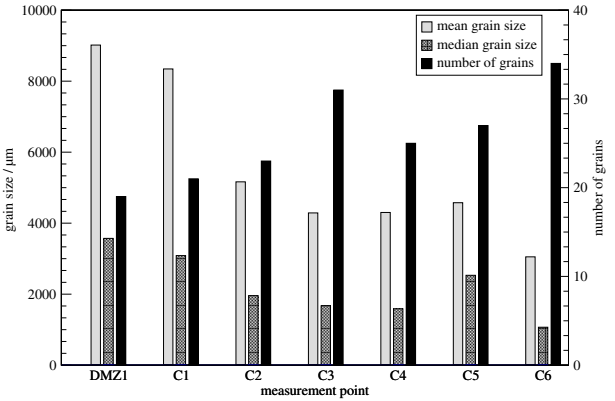

Figure 3: Mean and median grain sizes and number of grains at measurement points.

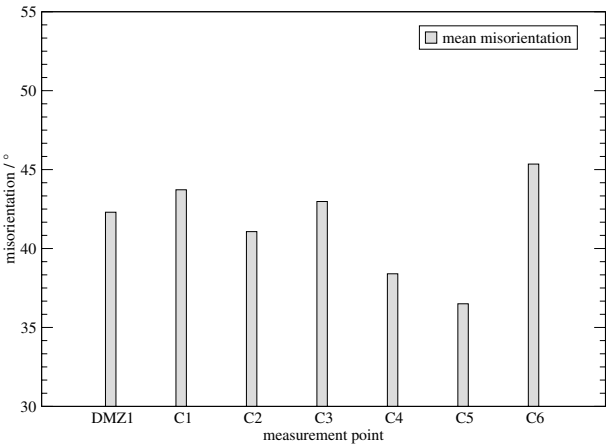

Figure 4: Mean misorientation at measurement points.

The histogram in Fig. 4 shows the statistical results of the misorientation distribution at the measurement points. Following the centre line of the block through to the die, the grains tend to align more and more in direction of the material flow. Hence, the misorientation angle generally decreases from point C1 up to point C6. The increasing value of point C6 located in the extrudate could be explained by static recrystallisation effects which can be sporadically observed in this zone. While interpreting the statistical results one should be aware that these values are based on single measurements where each EBSD data set covers only a region of 350 x 350 µm. Further measurements are planned to reduce statistical uncertainties.

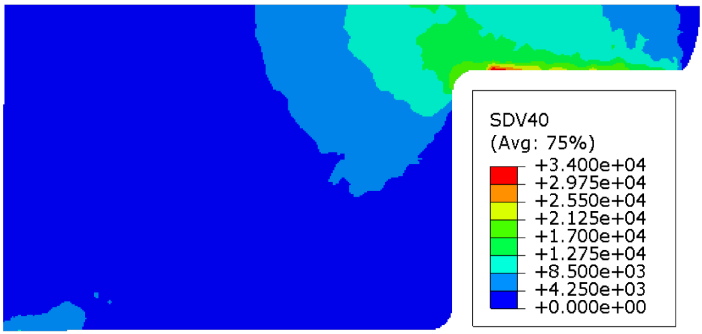

Figure 5: Simulated mean recrystallised grain size.

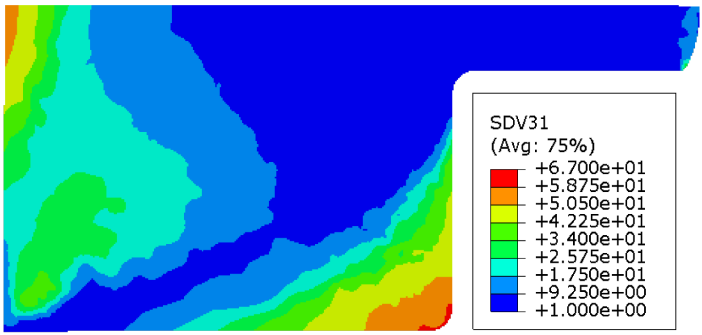

Figure 6: Simulated subgrain size.

3 Simulation

The simulation results presented in Fig. 5 and 6 are produced using a user material (UMAT) model implemented in the commercial Finite Element (FE) solver ABAQUS. The model is based on a formulation introduced by Sellars and Zhu [4] and can also be found in a similar form in [5, 6]. It describes the dependency of the inelastic part of the free energy density on the internal dislocation density, subgrain size, and grain misorientation. For a detailed overview of this model and its implementation refer [7]. In particular, the model is based on a flow rule depending on the Zener-Hollomon-Parameter [8].

Fig. 5 shows the distribution of the mean recrystallised grain size which mainly increases in the region near to the surface of the extrudate. This result corresponds to the general microstructure evolution described in section 2.1. The simulated subgrain size distribution presented in Fig. 6 shows a good qualitative correlation to the micrograph in Fig. 1. While the subgrain size in the DMZ remains near the starting value it significantly decreases in the SIZ which is also directly visible in the etched specimen.

Acknowledgement

This work is embedded into the Transregional Collaborative Research Centre TR30 (see http://www.transregio-30.com) funded and financially supported by the German Research Foundation (DFG).

References

[1] Bargel, H.J. & Schulze, G., *Werkstoffkunde*. Springer-Verlag: Berlin and Heidelberg, 1999.
[2] Saha, P., *Aluminum extrusion technology*. ASM International: Materials Park, Ohio, 2000.
[3] Humphreys, F.J. & Hatherly, M., *Recrystallization and Related Annealing Phenomena*. Elsevier: Oxford and Amsterdam, 2004.
[4] Sellars, C.M. & Zhu, Q., Microstructural modelling of aluminium alloys during thermomechanical processing. *Materials Science and Engineering A*, **280(1)**, pp. 1–7, 1985.
[5] T. Furu, G.J.B., H. R. Shercliff & Sellars, C.M., The influence of transient deformation conditions on recrystallization during thermomechanical processing of an al-1% mg alloy. *Acta Materialia*, **47(8)**, pp. 2377–2389, 1999.
[6] Sheppard, T., Prediction of structure during shaped extrusion and subsequent static recrystallisation during the solution soaking operation. *Journal of Materials Processing Technology*, **177(1-3)**, pp. 26–35, 2006.
[7] F. Parvizian, C.H., T. Kayser & Svendsen, B., Prediction of structure during shaped extrusion and subsequent static recrystallisation during the solution soaking operation. *Journal of Materials Processing Technology*, **209(2)**, pp. 876–883, 2009.
[8] Peng, Z. & Sheppard, T., Prediction of static recrystallisation after extrusion of shaped aluminium sections. *Materials Science Forum*, **467–470**, pp. 407–420, 2004.